Systems and Computers in Japan, Vol. 25, No. 1, 1994
Translated from Denshi Joho Tsushin Gakkai Ronbunshi, Vol. J76-D-II, No. 2, February 1992, pp. 350-358

Interactive 3-Dimensional Segmentation Method Based on Region Growing Method

Hiroyuki Sekiguchi* and Koichi Sano, *Members*

Systems Development Laboratory, Hitachi, Ltd., Kawasaki, Japan 215

Tetsuo Yokoyama, *Member*

Central Research Laboratory, Hitachi, Ltd., Kokubunji, Japan 185

SUMMARY

It has become easy to obtain three-dimensional (3D) data of the inside of the human body because of developments in X-ray computed tomography (CT) and magnetic resonance imaging (MRI). The 3D images of internal organs constructed from these data are useful in understanding the 3D shapes and positional relationships of the organs and are expected to be the diagnostic images of the next generation. However, many problems remain to be solved in making them practical, such as, improving the display speed of 3D images and implementing a 3D interface. For MRI, in particular, the difficulty in segmenting the display image is becoming a major impediment to the practical use of 3D MRI images. In this paper, we propose a practical segmentation method in which interactive corrective operations for 3D images are included in 3D region growing. To implement this method, we developed a 3D monitoring function for the segmentation process and an automatic function for removing the leaks generated during region growing. This method was applied to several 3D MRI data of the head and its effectiveness was confirmed.

Key words: 3D image segmentation; magnetic resonance image (MRI); "region growing"; technique.

1. Introduction

The 3D images of diseased areas are expected to be effective support for diagnosis. In clinics, because understanding the 3D position and shape of a diseased area is estimated from multiple two-dimensional cross-sectional images, understanding the 3D position and shape of the diseased area relies heavily on the reader's point of view and experience. By using 3D images, objective observations will be possible. In addition, 3D images are so easy to read that they will be ideal as tools for teaching or for explaining changes in diseased areas to patients.

Advances in X-ray CT and MRI measurement technologies in recent years have made 3D data acquisition possible. There is a great deal of activity in trying to construct 3D images from these data [1-5]. Recently, 3D images derived from X-ray CT data, in particular, have been put to practical use and used in clinical diagnosis. Because of the characteristics of X-rays, tissues which are easy to image like epidermis and bones are usually imaged for 3D images. On the other hand, MRI has the feature of being able to image with excellent contrast soft tissue like tumors which are difficult to display in X-ray CT. Therefore, we believe the need for 3D MRI images is substantial.

However, the difficulty in segmenting the target organ in the pre-processing for the 3D display of MRI images has slowed its being put to practical use. Seg-

*Presently, Kyoto University.

ISSN0882-1666/94/0001-0088

mentation of an X-ray CT primarily uses a gray level threshold. However, the gray level distributions of tissues overlap in an MRI image; therefore, segmentation based on a gray level threshold is not possible. The primary method has been to slice the 3D MRI data then have a person trace the contour of the organ on each slice. Naturally, this segmentation process took too much time and effort.

In addition to threshold and contour tracing segmentation methods, edge detection and region growing have been proposed. Edge detection finds candidate contour points of the target region by spatial differential processing, then connects these points to determine the contour of the region. Because of differentiating, this method has the flaw of being easily affected by noise. But processing is relatively simple, therefore, it is often used as the region extraction method for two-dimensional images. Still, the contours found in each slice must be connected to the preceding and following slices in a 3D image. Also, a region with a complex 3D shape is divided into several island regions in the slice; this necessitates a decision on whether the target is in each region. In any event, the application of edge detection to 3D images is not at all simple.

Region growing is a method to extract a whole region by expanding the region inside the target region by absorbing connected regions [6, 7]. The connectivity of regions is decided based on gray level differences between the whole target region and adjacent points or gray level differences between adjacent points. To perform the extraction with a high degree of reliability, a method has been proposed which includes edge information in the decision criteria [8]. However, suppressing leaks to the region's exterior which develop during region growing is limited by the decision criteria. Therefore, in many systems, high reliability is designed into the segmentation by introducing an interactive process. But this interactive processing is performed on each slice so the number of operations is proportional to the number of slices which are often numerous.

The method we propose involves interactive corrective processing based on 3D region growing. It differs from conventional methods in that interactive processing is not performed on the slices but on the 3D image. While manipulating 3D data on a two-dimensional display is generally problematic, this method is implemented with an automatic leak region extraction function which uses reverse region growing and a 3D monitor which monitors the segmentation process and allows the input of 3D coordinates.

Region growing is examined in detail in section 2. Section 3 describes the automatic leak region extraction algorithms and the 3D monitor which are the core of this method. The processing steps of the proposed method are explained in section 4. Then in section 5, the results of applying this method in 3D are described.

2. The Region Growing Algorithm

As illustrated in Fig. 1, region growing is a method where a whole target is extracted by growing a region by absorbing points connected to the target region. Figure 2 shows which adjacent points are absorbed. In 3D space, the 6 points in front, back, right, and above, and below a point, or the surrounding 26 points in the $3 \times 3 \times 3$ region are used. In either case, if the criteria are fulfilled the number of points grown increases in a progression, and there are almost no breaks in the growth caused by noise. In addition, regions with complicated 3D shapes can also be segmented since growth

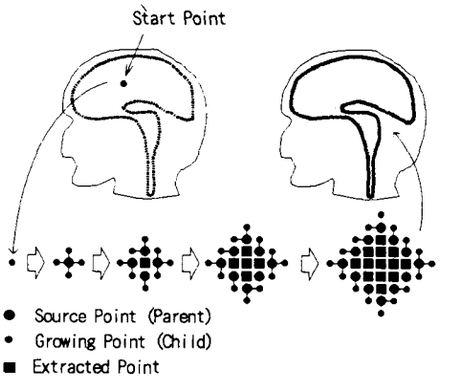

Fig. 1. Region growing algorithm.

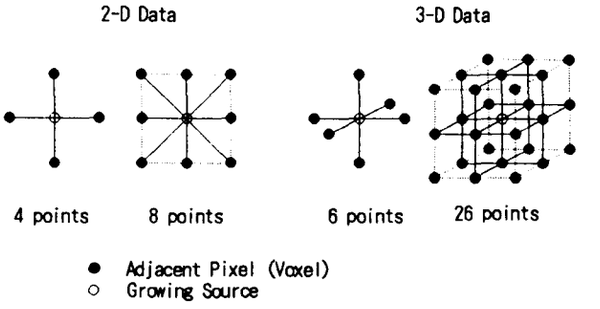

Fig. 2. Adjacent pixels (Voxels) of region growing.

is in all directions. But it has the flaw of stopping the region growing when leaks into the exterior are generated.

Although various criteria (growing criteria) in region connectivity have been considered, in this method, we use the growing criteria given by equation (1) which are based on the ideas of "the gray level of each pixel in the same region falls within some gray level range" and "the difference between adjacent pixels is small,"

$$|f_x - f_o| < \alpha \text{ and } |f_x - f_i| < \beta \qquad (1)$$

where f_i is the gray level of the point P_i extracted in the i-th growing; f_x is the gray level of a point adjacent to P_i; and f_o is the gray level of the start point P_o for the region growing. The parameters α and β establish the growing criteria and represent the tolerance to global changes in the gray level and the tolerance to local changes in the gray level, respectively. When a point P_x satisfies the above equation, P_x becomes extracted point P_{i+1} in the i + 1-st region growing.

Since typical data include noise and lack uniformity in gray levels, leaks to the outside are often generated. When the growing criteria are made more stringent in order to suppress leaks, extraction of the surrounding regions becomes difficult. Figure 3 illustrates how the segmented region grows for several growing criteria. By relaxing the criteria, segmentation reaches the region's periphery, but at the same time, the number of leaks to the outside increase. As a result, extracting the target region by only region growing is possible but is limited to the case where specific growing criteria are used for ideal data.

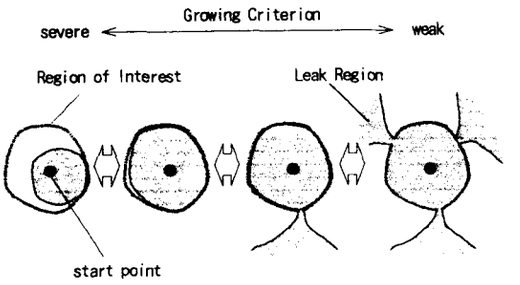

Fig. 3. Segmented regions under some circuits.

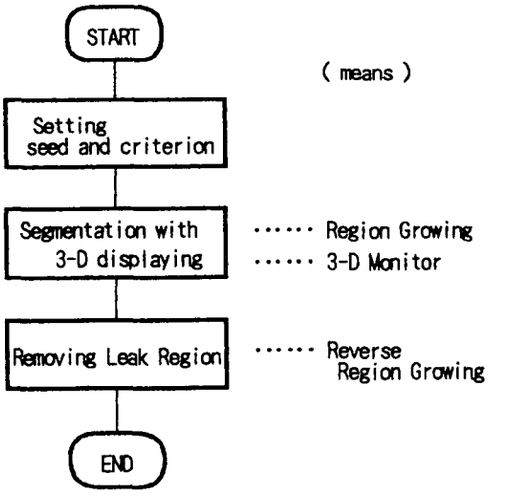

Fig. 4. Flowchart of the proposed method.

3. The Proposed Method

3.1. Overview

As explained in the previous section, the segmented region depends heavily on the growing criteria in region growing. Moreover, because of influences like nonuniformity in the gray levels and noise in real data, even when the growing criteria are thought to be optimum, either too much or too little of the target region is segmented, which is a problem. When the growing criteria are relaxed above some level, the size of the whole target region to be segmented will not change, because the boundary regions of the target region has large changes in gray level. In the proposed method, first, a region that includes the whole target region is segmented by using relaxed growing criteria, then the whole region is segmented by removing leak regions.

Figure 4 shows the flowchart of this method. In the first process, the region to be segmented is specified and the growing criteria are set. In the second process, the target region is segmented based on the region growing method explained in section 2. The third process removes leak regions generated during region growing. The reverse region growing algorithms and the 3D monitor which make up the procedure for leak region removal are described next.

3.2. Leak region removal

A key feature of this method is the efficient removal of the leak regions. A region growing method starting inside the leak region (reverse region growing

algorithm) was considered as the method to automatically extract and remove leak regions.

3.2.1. The principle of reverse growing

Although region growing is started from a leak region, extracting only the leak region are not possible. As explained in section 2, region growing is performed in all of the growing directions. Consequently, when region growing proceeds simultaneously in both the leak region and the target region, the two cannot be distinguished. However by adding the idea of "trace the segmentation times in reverse in the next region growing" to the growing criteria, the directionality of "leak region → connection → target region" in the growing direction can be presented. Hereafter, this region growing will be called reverse region growing. To trace the pixels based on their segmentation times, the previous region growing outputs the iteration number (i in equation (1)) as the result (see Fig. 6). Hereafter, we call this data "extraction history data."

When reverse region growing is started inside a leak region, after region growing progresses to some degree in the region, the speed of the region growing slows as a connection is approached. The number of points grown only in the connection becomes the number of pixels that form the connection. When the target region is entered after passing through the connection, region growing speeds up again. Figure 5 illustrates this aspect.

Several procedures that use this characteristic can be considered as the method for evaluating the connection, here, a connection is decided based on the ratio of N_i, the number of points grown at segmentation time i, to the average number of points grown during the m times preceding segmentation time i.

$$N_i/\{(N_{i+1}+N_{i+2}+\cdots+N_{i+m})/m\}>\gamma \qquad (2)$$

When the above equation is satisfied during reverse region growing, the point at segmentation time i + 1 is the connection. By accelerating region growing which is explained in the next section, since the number of points grown increases immediately after the connection is passed through, a rather large value (of at least 30) can be used in the γ criterion.

Since reverse region growing always moves towards the connection no matter where the start point is placed, the start point can be placed on the surface of the leak region. In this case, setting the start point on the 3D image (the removal region setting) becomes possible. This will be discussed in section 3.3.1.

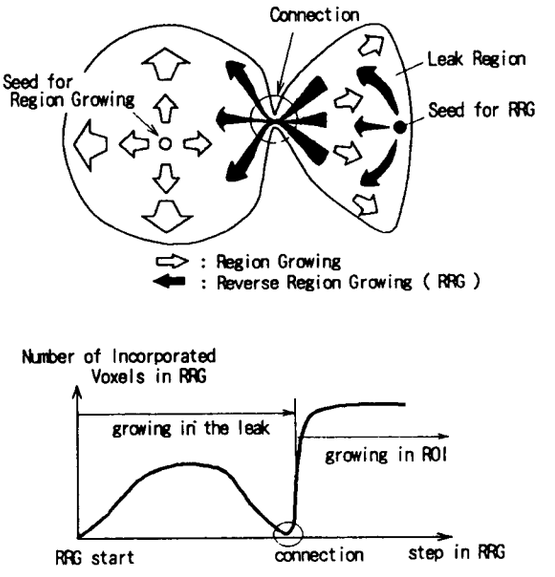

Fig. 5. The principle of reverse region growing.

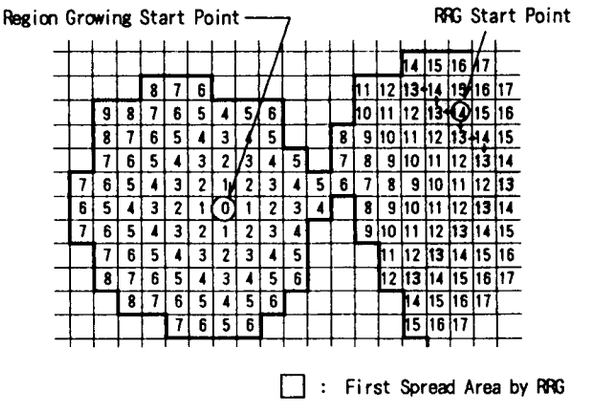

Fig. 6. Extraction history data (1).

3.2.2. Promoting region growing

As explained earlier, the connection is specified by the trend in the number of points grown during reverse region growing. Consequently, the larger the area in each segmented region, the clearer the convergence section; thus, specifying the connection becomes easy. However, because the "reverse trace of the segmentation times" criterion is particularly severe for region growing, the region does not spread much in normal region growing methods. As a result, growth proceeds by iterating from the region growing start point to the grown point.

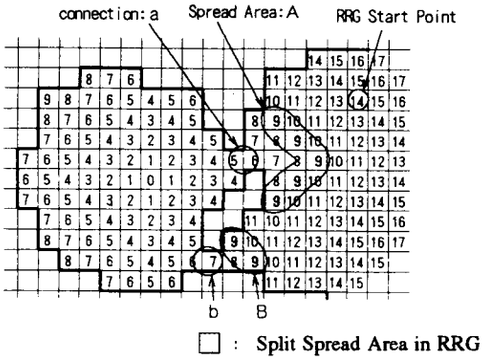

Fig. 7. Extraction history data (2).

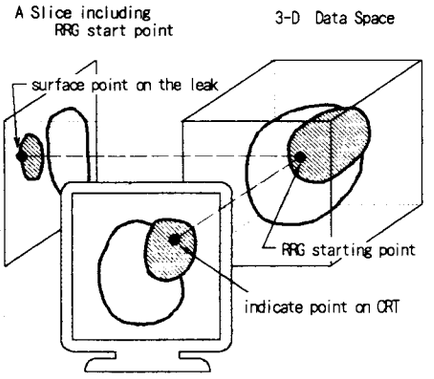

Fig. 8. Setting RRG start point using 3-D image on CRT.

Figure 6 shows the extraction history data when region growing was performed starting inside the target region. The numbers inside the boxes show the point in time (extraction time) when each pixel was extracted. Reverse region growing is performed from one point in the leak region on the right side. First, as the region growing start point, this point (extraction time 14) grows towards adjacent points at extraction time 13. Next, growth is towards points at extraction time 14 that are adjacent to the points at time 13. The region expands via this iteration. When no further expansion is possible, the growth step ends. The shaded sections in Fig. 6 indicate the region that was extracted at the end of this step (extraction time 13). With this extracted region as the origin for growth in the next step, the same growing process is performed.

When this growing method is used, the number of points grown increases instantly when the growing points enter the target region, thus, determining a connection point becomes easier.

3.2.3. When multiple leak regions exist

Practical data is not limited to generating only one leak. If each leak region is separated from the others, by performing reverse region growing for each region, the connecting points of each one can be specified. But when two leak regions connect to become one region as illustrated in Fig. 7, the two connections with different extraction times exist in these leak regions. In this case, the number of extracted points does not converge to one point, so specifying the connection points is no longer possible.

Specifically, when a leak region is formed from at least two regions, each region must be partitioned and its connection searched for. One region that is connected inside the growing portion is extracted in each growth step of reverse region growing, then this region becomes the seed for the next growth step. These connected regions can be extracted by using region growing with a growing criterion of "the extraction times are the same."

For example, the grown region is split into two parts at growing time 9 as illustrated by shaded parts in the data in Fig. 7. By performing reverse region growing in *'A'*, connection point *'a'* is sought, then, the leak region which includes point *'a'* is extracted and deleted. The remaining region *'B'* can be deleted in a similar manner as another leak region.

3.3. 3D monitor

3.3.1. The 3D monitor function

As explained in the previous section, reverse region growing is a function that automatically extracts specified leak regions. However, deciding which region to extract is very difficult to automate because anatomical knowledge is required. Therefore in this method, the extracted region is presented to the operator who makes the decision.

We can use slice images to verify the extracted region. But this is flawed because a number of slices must be referenced, and the 3D shape of the region is hard to understand. So in this method a 3D monitor was designed to display the extracted regions as 3D images. As well as being able to observe the region's spread in the 3D monitor, a 3D image is created at

each growth step because interactive processing at any time is possible. Moreover, 3D images from mulitple directions are displayed simultaneously to make it easy to find out the leak region.

The 3D monitor is also used as the procedure for acquiring the 3D coordinates of some region's surface. By indicating one point in a region on the monitor image, that point's 3D coordinate on the region's surface is obtained. Figure 8 shows the correspondence between the monitor image and the 3D data. The depth component of this coordinate is determined by referencing the value of the depth image (Z buffer) used in 3D generation. This coordinate is used as the start point for reverse region growing.

3.3.2. Rapid display on a 3D monitor

In order to continuously display the region growing process, 3D image generation requires real-time performance. In this section, we explain the acceleration method through more efficient image processing.

Known 3D display methods for voxel data are depth shading which shows depth image (Z buffer) itself and volume rendering [10] which uses the gray level gradient vectors. For both, most of the processing time is spent in the interpolation that accompanies data rotation and the voxel scan up to the surface of the target region to be displayed. Next, we will examine measures to address each of these.

(1) Limiting the rotation directions and the simultaneous multiple direction display

The purpose of the 3D monitor is not diagnosis, but to investigate the presence or absence of leaks. Consequently, a 3D display function from any direction is not always required; limiting the directions to front, back, left, and right is satisfactory. If the direction of rotation is limited to the direction perpendicular to the axis, interpolation becomes unnecessary because no position offsets from the grid points arise from the rotation. Enough of a speed margin is produced by eliminating interpolation, and simultaneously creating and displaying 3D images from multiple directions becomes possible.

(2) Creating and updating the depth image during region growing

In the 3D display process, the objects of the actual display calculations are only the voxels on the body's surface (hereafter, these are called surface voxels). But to specify these voxels, the voxels must be scanned in order from the front row. This represented a bottleneck to increasing the speed.

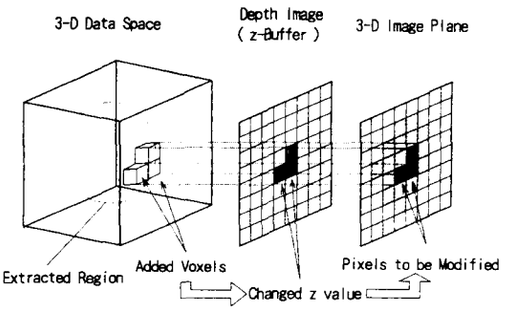

Fig. 9. Continuous displaying method for growing region.

While surface voxels are the voxels newly added during region growing, their coordinates are already known during region growing. As a result, by creating the depth image which corresponds to each projection direction from the surface voxels' coordinates (depth components) during region growing, voxel scanning during display becomes unnecessary. Furthermore, for this kind of continuously updated image, the whole image does not need to be rewritten, only the pixels that correspond to new surface voxels need to be updated as shown in Fig. 9. The image generation process can be accelerated by these methods and the region growing process can be continuously displayed.

4. Processing Procedure

4.1. Specifying the extraction region and setting the region growing criteria

(1) Specifying the extraction region

First, the start point for region growing is specified in the target extraction region. The geometric position of the start point is not considered to be particularly important. However, since its gray level value is used as the representative value of the target region's gray levels in the decision criteria (see Eq. (1)), the start point must be selected in the target region. Almost all of the interactive processing in this process is performed in the 3D image. Only this start point setting is performed on a slice that has the target gray level.

(2) Setting the region growing criteria

Table 1. Region growing criteria and extracted and leak regions

Criteria	α	β	Extracted region	Leak region
Strict	20	10	One part of region of interest (ROI)	None
↑	30	15	Major part of ROI	None
↑	40	20	All ROI	Leak in left eye socket
↓	50	25	All ROI	More of the top part of brain region
↓	60	30	All ROI	Closer to the right eye socket and brain stem
Weak	70	35	All ROI	Many leaks from the brain's surface

Parameters α and β are set in Eq. (1) of the region growing criterion. Parameter α shows the allowance for changes in the gray level from the representative gray level. When a region to be extracted has many gray level changes, a large α is used. Parameter β shows the allowance for gray level changes between adjacent points. When a region to be extracted has an ambiguous contour, a smaller β is used.

As explained in section 3.1, the region growing criteria used here are somewhat relaxed so that all the target regions are extracted even when many or few leaks are generated. In practice, the absence of the need to strictly set the region growing criteria is a major merit. However, if the criteria are too weak, many leaks will be generated and removing them is troublesome. Therefore, criteria with some degree of appropriateness for the target region must be set.

Suitable region growing criteria differ with the data to be used and the region to be extracted. When there are new data or unextracted regions, the parameters are set by repeated region growing trials.

4.2. Region extraction by region growing

After the start point and the region growing criteria have been set, the target region is extracted by region growing. During growth, the region is displayed on four simultaneous displays of the 3D image seen from the front, back, left, and right by the 3D monitor. The operator examines whether leaks are present from these images. The move to leak extraction can be performed when these regions become sufficiently large and the leaks are clearly recognized.

4.3. Deleting leak regions

When one point in a leak region in the monitor's region is indicated, processing moves to reverse region growing. As explained in section 3.3.1, the point on the leak region which corresponds to the indicated point becomes the start point for region growing. The connecting points between the leak region and target region are specified from the trend of points grown during reverse region growing. Then, the whole leak is extracted by region growing (forward direction) started from the connected points. The extracted leak region is displayed on the 3D image. After the operator's verification, it is deleted. When other leak regions exist, the same processing is performed and these regions are deleted.

5. Application to 3D MRI Data and Tests

Here, we use several 3D MRI data to examine the effectiveness of the proposed method. The MRI data was imaged by a Hitachi MRH-500 and is 128^3 voxels

of 3D data of a human head. The length of the side of a pixel is about 2 mm. Image processing was performed on a Stellar GS2000 graphics workstation which has a CPU performance of 20 MIPS and a 64-Mbyte main memory. The 3D data undergoes 3D smoothing beforehand to remove noise components. The objects to be extracted and used in diagnosis are the brain region, brain tissue, and a tumor.

First, tests for extracting the brain region are performed. When extraction is only by region growing, the relationships between the parameters α and β and the extracted region are listed in Table 1. This 3D data is ideal because a volunteer was used and enough time was taken for imaging. Nevertheless, the ability to extract just a sufficiently large region is limited to cases when the region growing criteria are $\alpha = 30$ and $\beta = 15$. The extraction is insufficient for more rigorous criteria, but leaks are generated for weaker criteria. Finding the optimum criteria is difficult during actual diagnosis. Therefore, the actual use is hypothesized and extraction is performed using weaker region growing criteria of $\alpha = 50$ and $\beta = 25$.

Figure 10 shows the leaks generated in the upper right region and left eye socket of the brain when the above criteria were used. When reverse region growing was performed in these regions, extraction and deletion were completed in each region in less that 1 minute. The results for both regions are shown in Fig. 11. Figure 11(b) shows the final extraction result. The operating time for the whole extraction process lasted about 10 minutes. A cross section of the extraction result is shown in Fig. 12. We see that the brain region was extracted to almost its boundary.

Because the ventricle and the tumor have a smaller volume than the brain region, their extraction times were shorter than that of the brain region. As shown in Fig. 13(a), when the ventricle, a region with low gray levels, is extracted, leaks are always generated through the hollow part with the same low gray levels. As a result, the deletion of unneeded regions by reverse region growing becomes essential. Figure 13(b) shows the result after the leaks were deleted. On the other hand, a tumor is displayed at higher gray levels due to the action of contrast media, so extraction was possible only by ordinary region growing. Figure 13(c) shows the result of the extracted tumor and ventricle superimposed on the brain region.

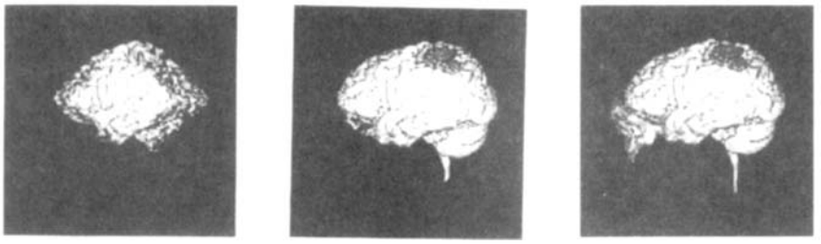

(a) Growing in the ROI (b) Two Leaks occured (c) Growing in the Leak

Fig. 10. Extraction processing using region growing.

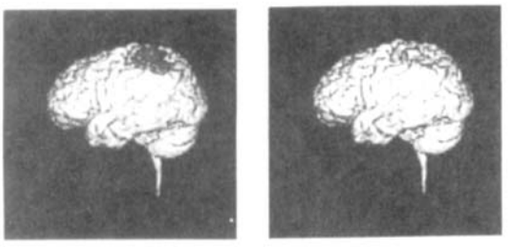

(a) Removing Leak (lower left) (b) Removing Leak (upper right)

Fig. 11. Removing leaks using reverse region growing.

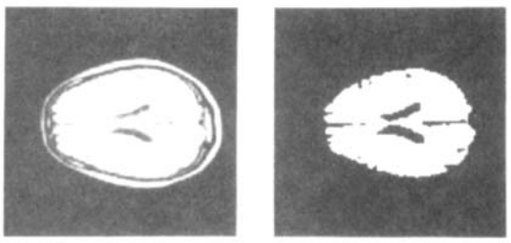

(a) Original Slice (b) Processed Slice

Fig. 12. Checking of the segmentation result by slice image.

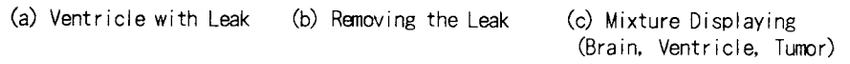

Fig. 13. Applying proposed method to patient data.

6. Conclusions

A practical region segmentation method was proposed for 3D MRI data. Although some degree of image recognition processing in the extraction process for MRI data was required, the image recognition power of current computers has not reached a practical level. Fast, highly reliable extraction is implemented through effective human support for an extraction process performed by computer.

In a method like this one which includes interactive operations, its practicality is primarily influenced by the suitability of the operations and the amount of work. By automatically eliminating leak regions by reverse region growing and having a man-machine interface for 3D images in this method, convenient operation and a light work load were realized.

The biggest defect in conventional region growing is leaks grown without limit from minute connections. In contrast, reverse region growing uses the smallest of these connections to remove leaks. We now consider an effective way to eliminate the defects of region growing.

When this method was used on 128^3 data for extraction, the brain region can be extracted in about 10 minutes, and the ventricle and the tumor in about 2 to 3 minutes. The interactive operation is a simple way to indicate one point on a 3D image. Moreover, the number of operations do not depend on the number of data slices. The extraction method explained in this paper is a highly practical method at this time.

However, in order to specify the connections in this algorithm, the target region to be extracted must have some minimum volume. Consequently, when extracting objects with fine shapes like blood vessels and nerves, assistance like having a person indicate the connections becomes necessary.

In the future, the aims include to further examine the region growing criteria while preserving the reliability of the extraction and to promote more automation.

Acknowledgment. We would like to thank Jun Takane and Hideaki Koizumi of the Measurement Equipment Department, Hitachi Central Research Laboratory for their cooperation in providing the measurement equipment for 3D MRI data used in this research. We also thank Kazuhumi Ito, assistant hospital administrator at Hitachi General Hospital, and Kazuya Sukegawa for providing clinical data.

REFERENCES

1. K. Koyama, Y. Matsuoka, J. Nishikawa and M. Ito. 3D Images Using CT and MR Images. Image Information, **21**, 17, pp. 821-827 (Aug. 1989) (in Japanese).
2. S. Abo and H. Sekiguchi. Solid Cross Sections and 3D Display System Using 3D Image Memory. Transactions of the Institute of Electronics, Information and Communication Engineers (D-II), **J72-D-II**, 4, pp. 577-585 (April 1989) (in Japanese).
3. S. Yokoi. Display Technique for 3D Medical Images. Journal of the Japan Society of Medical Electronics and Biological Engineering, **3**, 8, pp. 11-17 (Aug. 1989) (in Japanese).
4. N. Niki, Y. Kawata and H. Sato. 3D Display Techniques for Medical Images with Ambiguous Shapes. Transactions of the Institute of Electronics, Information and Communication

Engineers (D-II), **J73-D-II**, 10, pp. 1707-1715 (Oct. 1990) (in Japanese).
5. K. Sano. Image Processing Technology in Medical Care. Transactions of the Society of Instrument and Control Engineers, **28**, 7, pp. 579-587 (July 1989).
6. A. Rosenfeld and A. C. Kak. Digital Picture Processing, 2nd edition, **2**, pp. 138-145 (1982).
7. J. Toriwaki and H. Suzuki. Analysis and Recognition of 3D Medical Images. Journal of the Japan Society of Medical Electronics and Biological Engineering, **3**, 8, pp. 18-26 (Aug. 1989) (in Japanese).
8. H. Koh, H. Suzuki and J. Toriwaki. A Segmentation Method Using Region Information and Edge Information. Transactions of the Institute of Electronics, Information and Communication Engineers (D-II), **J74-D-II**, 12, pp. 1651-1660 (Dec. 1990) (in Japanese).
9. H. Sekiguchi, K. Sano and T. Yokode. A Proposal for Organ Segmentation Suited to Volume Rendering. Proceedings of the 9th Annual JAMIT Conference, **8**, 3, pp. 233-234 (July 1990) (in Japanese).
10. M. Levoy. Display of Surfaces from Volume Data. IEEE CG&A, **8**, 3, pp. 29-37 (May 1988).

AUTHORS (from left to right)

Hiroyuki Sekiguchi received a B.E. in electronics in 1986 and an M.E. in 1988 from Kyoto University. In 1988, he entered Hitachi Seisakusho where he performed research on medical image processing in the Systems Development Laboratory. He is currently an Assistant Professor in the Applied Systems, Faculty of Engineering, Kyoto University.

Koichi Sano received a B.E. in systems engineering in 1976 and an M.E. in 1978 from Kobe University. In 1978, he entered the Systems Development Laboratory, Hitachi Seisakusho. His research interests are medical information processing systems and medical image processing. He is a member of the IEEE, the Japan Society of Medical Electronics and Biological Engineering, the Magnetic Resonance Medical Society of Japan, and the Society of Instrument and Control Engineers of Japan.

Tetsuo Yokoyama received a B.S. in health in 1970 from the Faculty of Medicine and an M.S. in 1972 from the University of Tokyo. He later received a doctorate in health from the University of Tokyo. He entered Hitachi Seisakusho in 1972 and is involved in research and development in medical information processing and image processing. Dr. Yokoyama is currently head of the Medical Electronics Research Center, Central Research Laboratory, Hitachi Ltd. He is a member of the IEEE, the Japan Society of Medical Electronics and Biological Engineering, and the Society of Instrument and Control Engineers of Japan.